

**Supplementary Materials:**

**Spinel FeNi<sub>2</sub>S<sub>4</sub> with rich sulfur vacancies grown on reduced graphene oxide  
toward enhanced supercapacitive performance**

Yingrui Tao,<sup>a,§</sup> Jingjing Yuan,<sup>a,b,§</sup> Xingyue Qian,<sup>a</sup> Qi Meng,<sup>a</sup> Junwu Zhu,<sup>b</sup> Guangyu

He<sup>\*a</sup> and Haiqun Chen<sup>\*a</sup>

<sup>a</sup> Key Laboratory of Advanced Catalytic Materials and Technology, Advanced Catalysis and Green Manufacturing Collaborative Innovation Center, Changzhou University, Changzhou, Jiangsu Province, 213164, China.

<sup>b</sup> School of Chemical Engineering, Nanjing University of Science and Technology, Nanjing, Jiangsu 210094, China.

<sup>§</sup>Y. Tao and J. Yuan contributed equally.

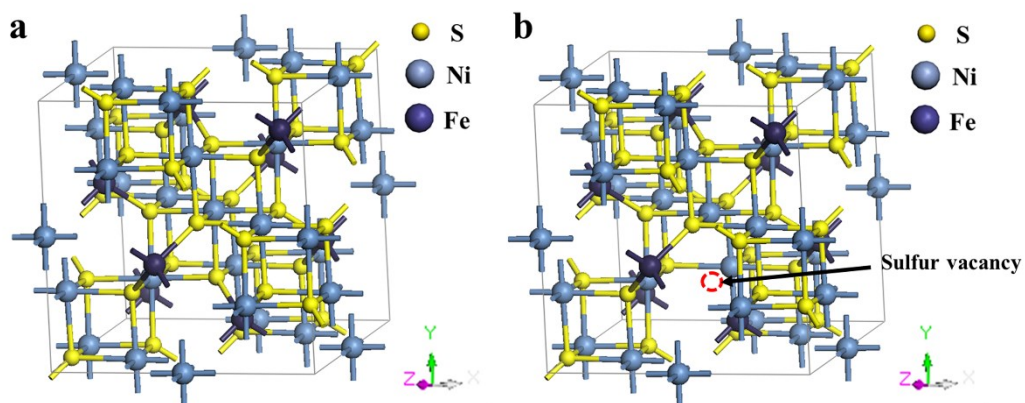


**Fig. S1** The structural models of (a)  $\text{FeNi}_2\text{S}_4$  and (b)  $\text{r-FeNi}_2\text{S}_4$ .

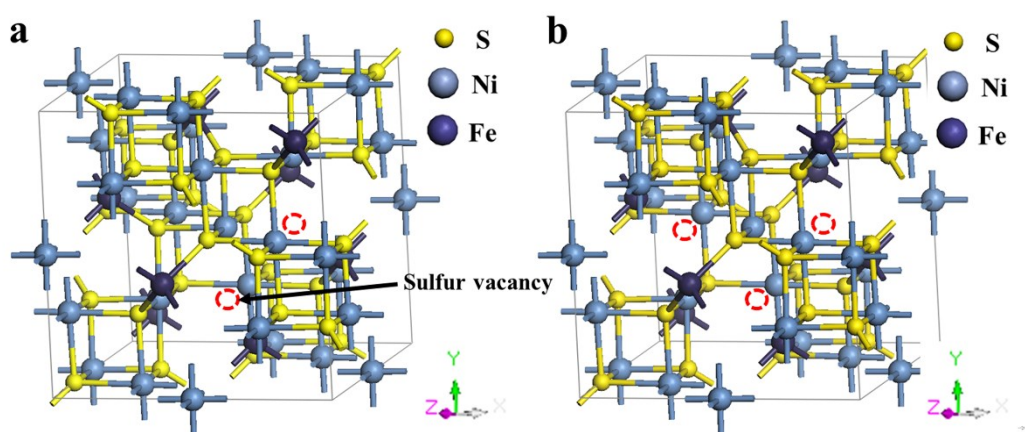


**Fig. S2** The structural models of (a)  $\text{r-FeNi}_2\text{S}_{4-2}$  and (b)  $\text{r-FeNi}_2\text{S}_{4-3}$ .

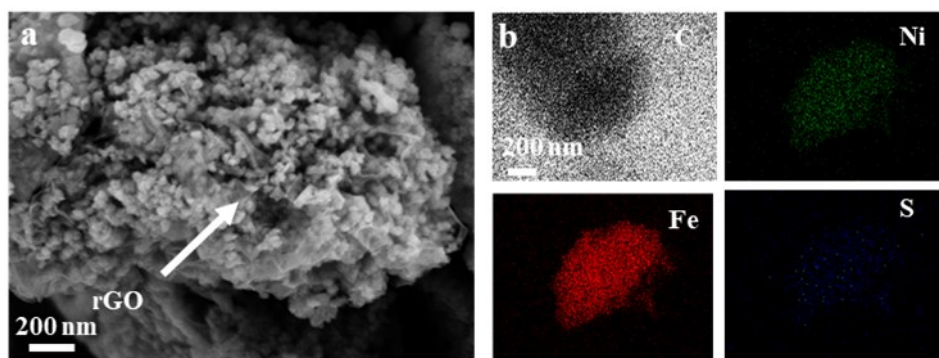


**Fig. S3** (a) FESEM image and (b) element mappings of FeNi<sub>2</sub>S<sub>4</sub>-rGO.

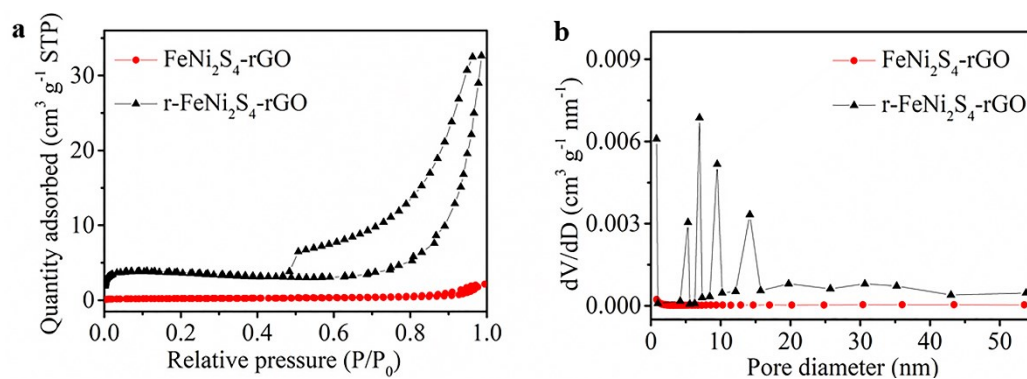


**Fig. S4** (a) N<sub>2</sub> adsorption-desorption isotherms and (b) pore-size distribution of

FeNi<sub>2</sub>S<sub>4</sub>-rGO and r-FeNi<sub>2</sub>S<sub>4</sub>-rGO.

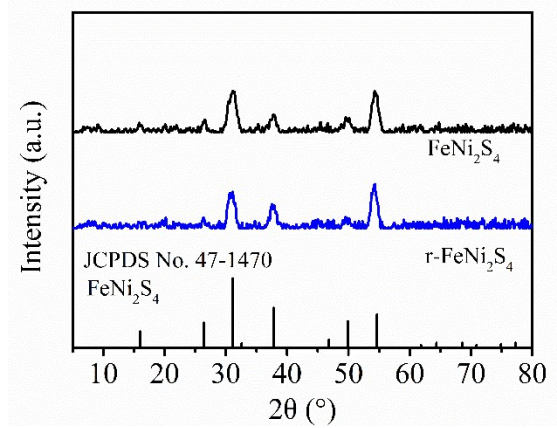


**Fig. S5** XRD patterns of  $\text{FeNi}_2\text{S}_4$  and  $\text{r-FeNi}_2\text{S}_4$ .

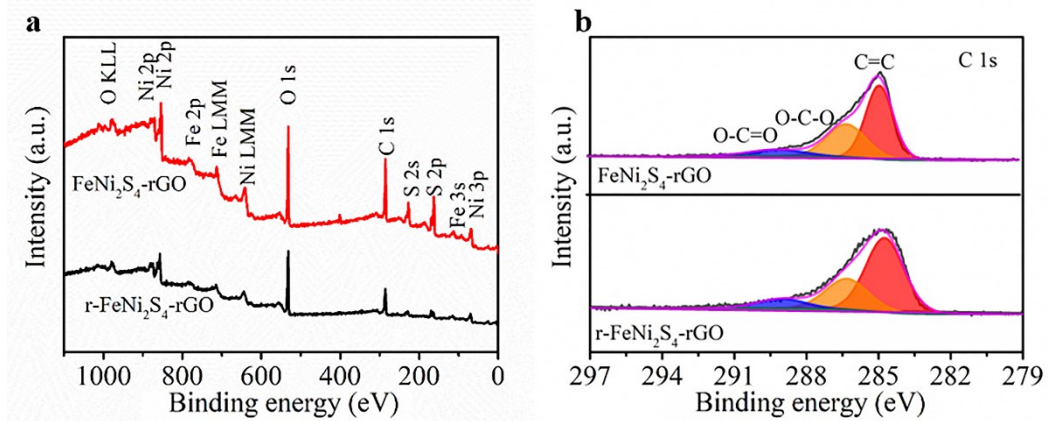


**Fig. S6** (a) XPS survey spectra and (b) C 1s XPS spectra of  $\text{FeNi}_2\text{S}_4\text{-rGO}$  and  $\text{r-FeNi}_2\text{S}_4\text{-rGO}$ .

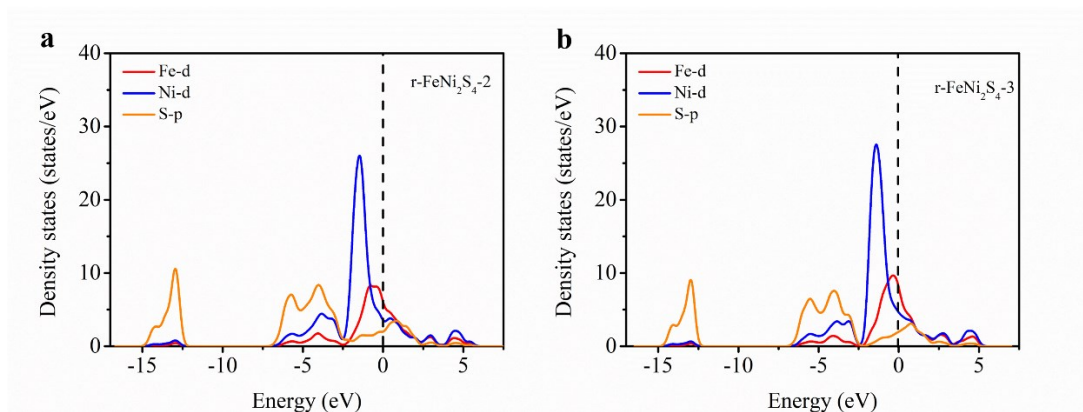


**Fig. S7** Projected density of states for r-FeNi<sub>2</sub>S<sub>4</sub>-2 and (b) r-FeNi<sub>2</sub>S<sub>4</sub>-3.

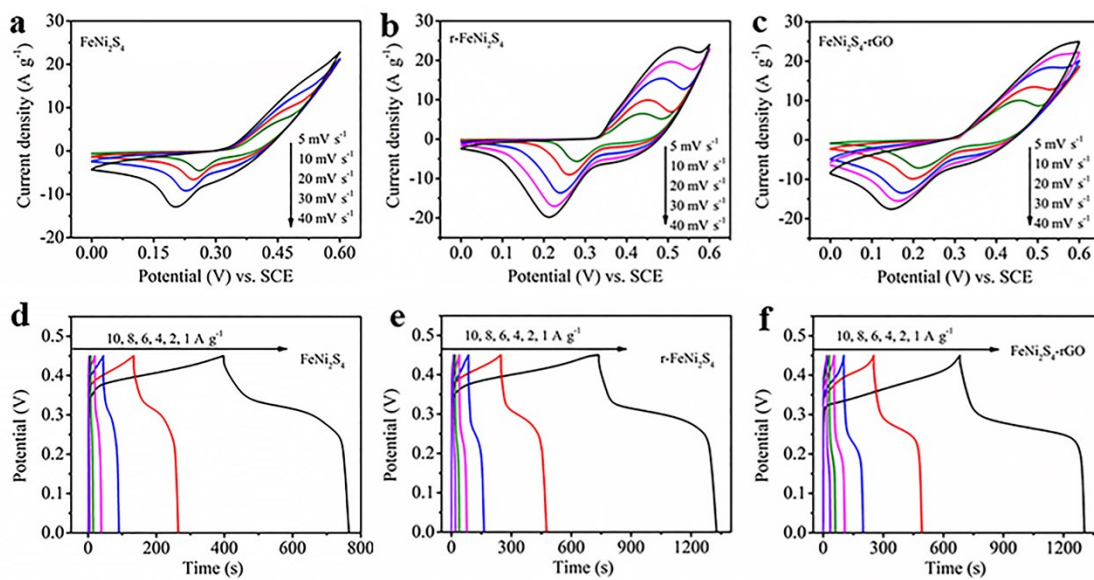


**Fig. S8** CV curves of (a) FeNi<sub>2</sub>S<sub>4</sub>, (b) r-FeNi<sub>2</sub>S<sub>4</sub> and (c) FeNi<sub>2</sub>S<sub>4</sub>-rGO at various scan rates (5~40 mV s<sup>-1</sup>). GCD profiles of (d) FeNi<sub>2</sub>S<sub>4</sub>, (e) r-FeNi<sub>2</sub>S<sub>4</sub> and (f) FeNi<sub>2</sub>S<sub>4</sub>-rGO at different current densities (1~10 A g<sup>-1</sup>).

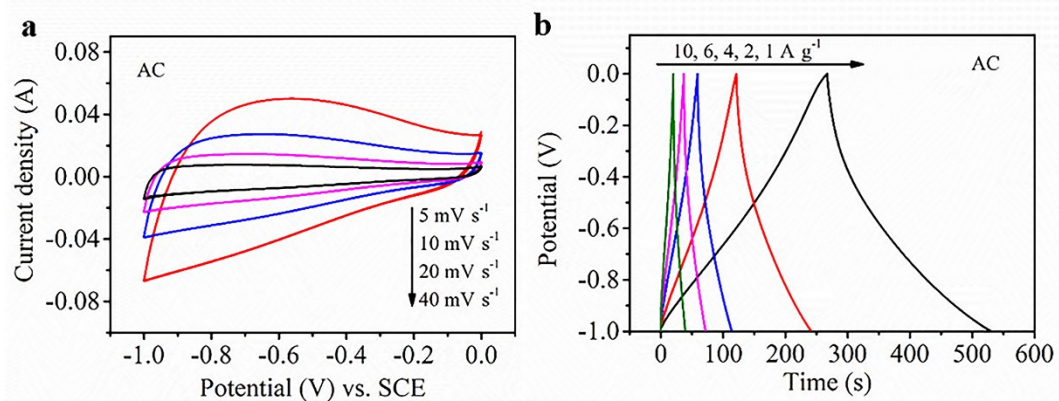


**Fig. S9** (a) CV curves of AC at various scan rates (5~40 mV s<sup>-1</sup>) and (b) GCD profiles of AC at different current densities (1~10 A g<sup>-1</sup>).

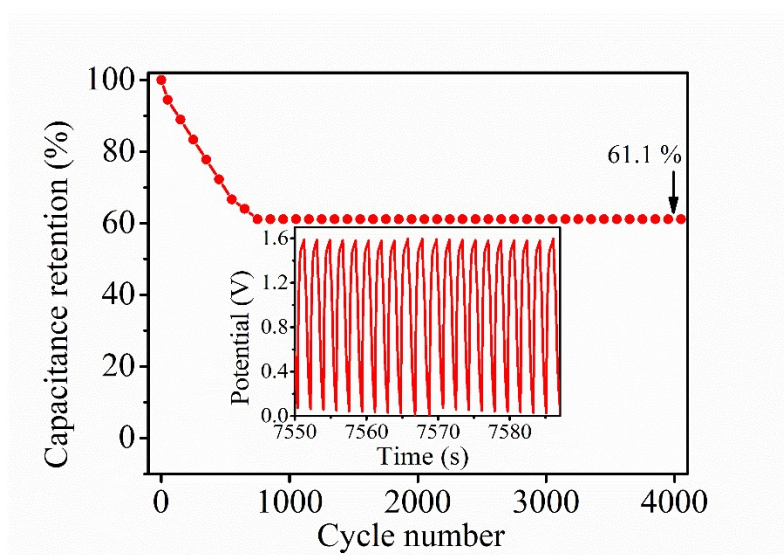


**Fig. S10** Cycling performance of r-FeNi<sub>2</sub>S<sub>4</sub>-rGO//AC at 10 A g<sup>-1</sup> after 4000 cycles, the inset shows part of the GCD profiles at the current density.